Eigenmodes of a hydrodynamically coupled micron-size multiple-particle ring

R. Di Leonardo,[1] S. Keen,[2] J. Leach,[2] C. D. Saunter,[3] G. D. Love,[3] G. Ruocco,[1] and M. J. Padgett[2]
[1]*INFM-CRS SOFT, c/o Universitá di Roma "La Sapienza," I-00185 Roma, Italy*
[2]*SUPA, Department of Physics & Astronomy, University of Glasgow, Glasgow, G12 8QQ, United Kingdom*
[3]*Department of Physics, Durham University, Durham, DH1 3LE, United Kingdom*
(Received 17 July 2007; revised manuscript received 21 September 2007; published 26 December 2007)

We use a continuous acquisition, high-speed camera with integrated centroid tracking to simultaneously measure the positions of a ring of micron-sized particles held in holographic optical tweezers. Hydrodynamic coupling between the particles gives a set of eigenmodes, each one independently relaxing with a characteristic decay rate (eigenvalue) that can be measured using our positional data. Despite the finite particle size, we find an excellent agreement between the measured eigenvalues and those numerically predicted by Oseen theory applied to the two-dimensional (2D) ring geometry. Particle motions are also analyzed in terms of the alternative eigenmode set obtained by wrapping onto the ring the eigenmodes of a 1D periodic chain. We identify the modes for which the periodic chain is a good approximation to the ring and those for which it is not.

DOI: 10.1103/PhysRevE.76.061402 PACS number(s): 82.70.−y, 81.05.−t

The dynamics of colloidal suspensions are extremely important in both industrial and biological applications [1]. Hydrodynamic interactions play a crucial role in the dynamics of suspended bodies and, due to their long range, are a challenging problem to tackle with theoretical and numerical tools. Though the two body problem can be solved theoretically, many-body effects are still at the center of active debate [2]. Moreover, since hydrodynamic couplings are always present, the ability to accurately describe their behavior is crucial for the correct interpretation of various dynamical phenomena involving many particles suspensions, i.e., when probing elastic response of colloidal crystals [3–5], or the diffusion of colloidal particles in confined geometries [6–9].

Until recently, rather than individual particles, experimental studies mainly focused on bulk properties. Optical tweezers [10] have been used to investigate hydrodynamic interactions in two particle systems [11] and to investigate the coupling of particles to surfaces [12]. Meiners *et al.* [11] used quadrant photodiodes [13] to make rapid measurements of the particle positions. After many minutes of averaging the time-dependent cross correlations showed an anticorrelated dip. This arises because the antisymmetric motion eigenmodes are more highly damped than the symmetric ones and hence negative correlations persist longer. Similar work has studied the hydrodynamic coupling between oscillating particles in optical tweezers [14].

Recently, Polin *et al.* reported the use of a video camera to simultaneously measure the positions of several particles trapped in a linear chain, comparing their correlated motion to the predicted results for an infinite chain [15]. A water-glycerol mixture was used as the solvent to slow down dynamics to a time scale accessible to a conventional video camera. Their aim was to investigate the possibility of observing anomalous dispersion relation for the chain dynamics, concluding that to observe propagating modes one has to resort anyway to low viscosity solvents and high trap stiffness. There is another good reason to find methods to study multiparticle hydrodynamic correlations in low viscous solvents. A system of N hydrodynamically coupled damped oscillators is characterized by a spectrum of decay rates in the correlation matrix whose typical relative splittings are of order a/rN with a particle radius and r interparticle distance. It can be shown that for a Gaussian random process with a self-correlation function decaying with rate Γ, the relative error on Γ goes as the inverse square root of the total number of sample points. Therefore to resolve the fine structure of eigenvalues of an ensemble of order ten particles at a few diameters distance we need to collect some 100 000 samples or equivalently about three hours acquisition at a standard frame rate of 25 fps, raising concerns over contamination of the sample by free particles and stability of the optical trap system.

As an alternative to quadrant diodes or viscosity control, we use a high-speed video camera to monitor many particles optically trapped in water. Commercial cameras can take images at 10 s of kHz, typically writing images to a buffer before downloading onto a computer. Unfortunately, onboard memory limitations restrict measurement to a few seconds, insufficient for distinguishing correlations against a random noise background.

One application driving real-time, high-speed image acquisition is adaptive optics, where cameras are needed to record wave-front data at rates up to several kHz. A Shack-Hartmann wave-front sensor employs a microlens array to generate a matrix of spots on an imaging array. Any local inclination of the incident wave front causes a lateral displacement of the corresponding spot [16]. To enable continuous monitoring, high-speed "smart cameras" are being developed with integrated signal processing, where a programmable logic array measures the position of each spot [17]. In this work we use one such camera to image multiple trapped particles and track their positions. Since it is only the positional information which is transferred, rather than the whole image, the bandwidth of the interface is high enough for indefinite monitoring of the position of many particles.

We holographically trap eight 2 μm particles in a ring and analyze their motion in terms of the predicted eigenmodes. Using the Oseen approximation we numerically calculate the eigenvalue (i.e., damping) spectrum of the eigenmodes predicted for a ring, and compare this to that analytically calculated for a periodic one-dimensional (1D) linear chain. Holographic optical tweezers are now routinely

 ©2007 The American Physical Society

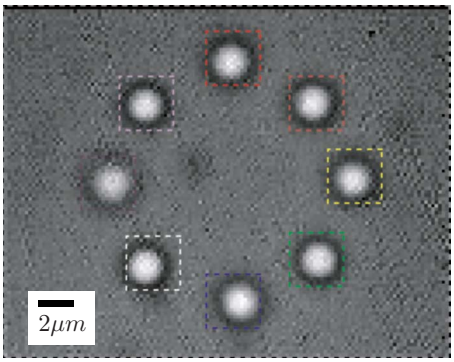

FIG. 1. (Color online) Ring of eight particles held by optical tweezers. The squares show regions of interest within which the particles' positions were monitored using a high speed camera.

used for dynamic control of multiparticle arrays in two [18] and three dimensions [19–21]. Our system uses a spatial light modulator (SLM, HoloEye LCR 2500) placed in the Fourier plane of the sample. The trapping laser (Opus, LaserQuantum) emits up to 2.0 W at 532 nm, which after diffraction from the SLM and transmission through the 1.3 NA ×100, Plan Neofluar objective lens, resulted in 500 mW distributed between the optical traps.

The hologram kinoform was calculated using a modified [22] Gerchberg-Saxton algorithm [23]. Eight 2 μm diameter silica beads were suspended in water and trapped to form a ring, approximately 25 μm above the cover slip. The particle positions were continuously measured using a center of mass algorithm on background subtracted images, Fig. 1, with an accuracy of order 10 nm [24,25]. The x-y positions for the trapped particles were continuously logged over several minutes.

To model the anticipated behavior of the ring we describe a generic two-dimensional configuration of N particles through the $2N$ array $\mathbf{R}$ with components R_i^α $(i=1,\ldots N,\ \alpha=1,2)$. Neglecting inertial terms, the equation of motion in the presence of an external force field $\mathbf{F}$ takes the form [26]

$$\dot{\mathbf{R}} = \mathbf{H}(\mathbf{R}) \cdot \mathbf{F}. \tag{1}$$

In the large interparticle separation limit the mobility matrix $\mathbf{H}$ can be approximated by the Oseen tensor [27],

$$H_{ij}^{\alpha\beta} = \frac{1}{\gamma_0}\delta_{\alpha\beta}\delta_{ij} + \frac{1}{\gamma_0}(1-\delta_{ij})\frac{3}{4}\frac{a}{\mathrm{r}_{ij}}\left(\delta_{\alpha\beta} + \frac{r_{ij}^\alpha r_{ij}^\beta}{\mathrm{r}_{ij}^2}\right), \tag{2}$$

where γ_0 is the drag coefficient $6\pi\eta a$, the particle separation is $r_{ij}^\alpha = R_j^\alpha - R_i^\alpha$, r_{ij} is its modulus, and δ is the Kronecker delta.

We can separate the external forces into the trapping forces, $-\mathbf{K}\cdot\delta\mathbf{R}$, elastically restoring particle positions to $\mathbf{R}^0$, and the stochastic forces $\mathbf{S}$ that have a vanishing average and which are uncorrelated with system configuration at any previous time. Introducing the displacement coordinates $\delta\mathbf{R} = \mathbf{R} - \mathbf{R}^0$ we can rewrite Eq. (1):

$$\delta\dot{\mathbf{R}} = \mathbf{H}(\mathbf{R}) \cdot [-\mathbf{K}\cdot\delta\mathbf{R} + \mathbf{S}]. \tag{3}$$

The equilibrium distribution function for $\delta\mathbf{R}$ is

$$P(\delta\mathbf{R}) = \frac{1}{(2\pi)^{3N/2}\det(\mathbf{K}^{-1})}\exp\left[-\frac{\mathbf{K}:\delta\mathbf{R}\,\delta\mathbf{R}}{2k_BT}\right], \tag{4}$$

where the covariance matrix is

$$\langle \delta\mathbf{R}\,\delta\mathbf{R}\rangle = k_BT\mathbf{K}^{-1}. \tag{5}$$

The high trap strength ensures that particle displacements from equilibrium positions are small compared to interparticle distances and we can assume

$$\mathbf{H}(\mathbf{R}) \simeq \mathbf{H}(\mathbf{R}^0) = \mathbf{H}^0. \tag{6}$$

Substituting Eq. (6) into Eq. (3) and multiplying on the right by $\delta\mathbf{R}(0)$, we obtain after statistical averaging

$$\langle \delta\dot{\mathbf{R}}(t)\,\delta\mathbf{R}(0)\rangle = -\mathbf{H}^0\cdot\mathbf{K}\cdot\langle\delta\mathbf{R}(t)\,\delta\mathbf{R}(0)\rangle \tag{7}$$

or, in a more compact form,

$$\dot{\mathbf{C}}(t) = -\boldsymbol{\Gamma}\cdot\mathbf{C}(t), \tag{8}$$

where we have introduced the matrices $\mathbf{C}(t) = \langle\delta\dot{\mathbf{R}}(t)\,\delta\mathbf{R}(0)\rangle$ and $\boldsymbol{\Gamma} = \mathbf{H}^0\cdot\mathbf{K}$.

Equation (8) represents a system of coupled linear first order differential equations with initial conditions (5). The formal solution is

$$\mathbf{C}(t) = e^{-\boldsymbol{\Gamma}t}\cdot\mathbf{C}(0). \tag{9}$$

Since $\boldsymbol{\Gamma}$ is a symmetric matrix we can diagonalize it, finding an orthonormal basis set. Calling $\mathbf{e}_m$ the eigenmodes and λ_m the corresponding eigenvalues we can rewrite Eq. (9) in the eigencoordinates $Q_m = \mathbf{e}_m\cdot\delta\mathbf{R}$,

$$\mathbf{D}(t)\cdot\mathbf{D}^{-1}(0) = e^{-\boldsymbol{\Lambda}t}, \tag{10}$$

where

$$D_{mn}(t) = \langle Q_m(t)Q_n(0)\rangle, \tag{11}$$

$$\Lambda_{mn} = \delta_{mn}\lambda_m. \tag{12}$$

For identical traps and vanishing hydrodynamic interactions $(a/r\to 0)$, the diagonal elements $\boldsymbol{\Gamma}$ would be k/γ_0, i.e., the autocorrelation decay rate of the isolated particles, and all of the off-diagonal elements would be zero.

The hydrodynamic interaction between the particles in the ring couples their motion. The off-diagonal terms are no longer zero but can be calculated from Eq. (2). Diagonalization of this matrix gives the eigenvalues, i.e., the decay rates of the independent eigenmodes. Alternatively, the eigenmodes of a periodic chain are known to be simple sine and cosine functions for both lateral and axial modes with periods that are rational fractions of the chain period and a short wavelength cutoff determined by the particle spacing. The corresponding eigenvalues are readily calculated by inserting these eigenmodes into Eq. (3), using Eq. (2) again to calculate the coupling terms.

Figure 2 shows the predicted eigenmodes for an eight particle ring, the known eigenmodes for the periodic chain, and how these modes map onto a ring. As with earlier work [15] we analyze our observations in terms of predicted eigenmodes and check that the basis set decouples the fluctuations

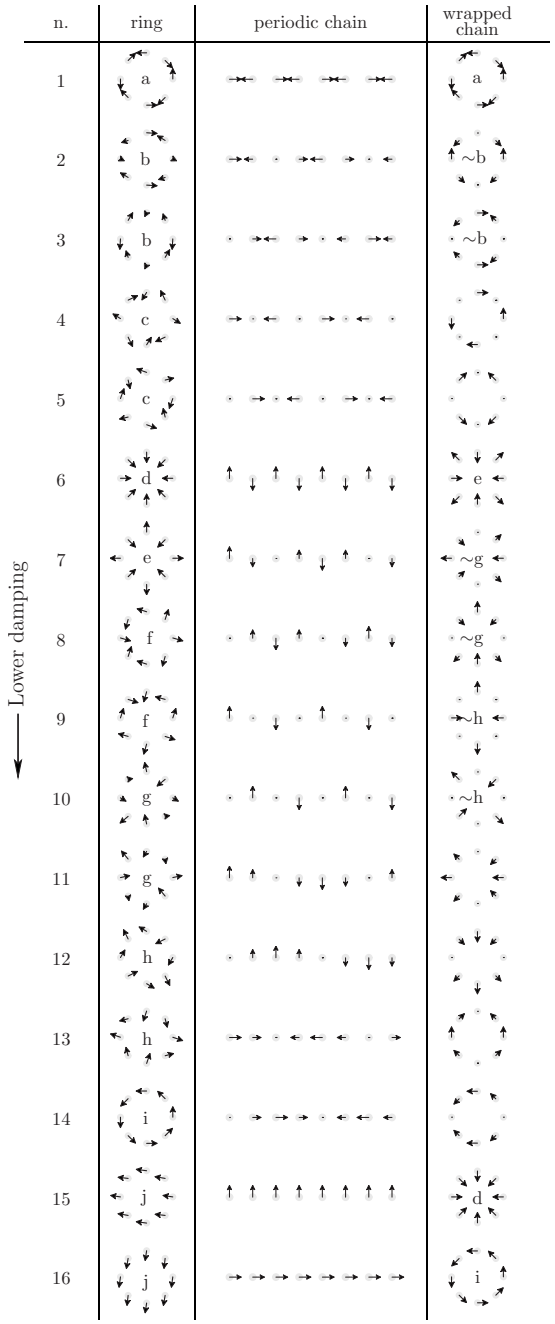

FIG. 2. The 16 eigenmodes predicted using the Oseen approximation for the ring, a periodic 1D chain, and the chain coordinate mapped onto a ring. The ring eigenmodes are labeled a–j with (*) denoting degeneracy. These modes are cross referenced to those of the periodic chain, many of which occur in a different position within the eigenmode spectrum.

as a self-correlation of eigencoordinates that can be fitted with a single exponential and where the cross correlations are negligibly small.

Figure 3 shows the measured autocorrelation functions of the eigenmodes of the eight particle system numerically analyzed as a ring and analytically analyzed as a 1D periodic chain. The straight line nature of log plot, together with the absence of significant cross correlations, confirms that both

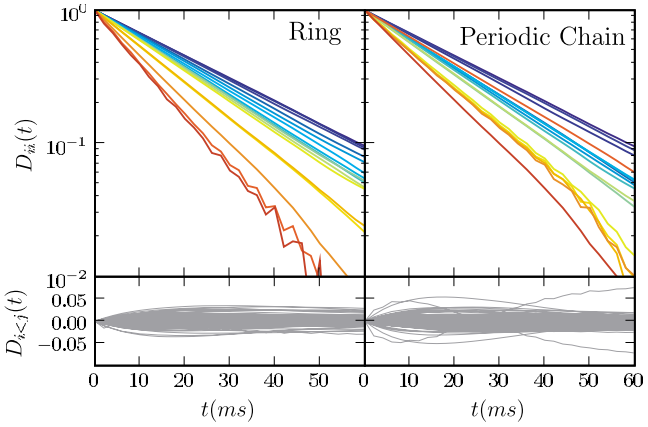

FIG. 3. (Color online) The 16 measured autocorrelation functions for the predicted eigenmodes for the eight particle ring and the eight particle periodic chain. The slowest decaying eigenmodes correspond to common motion of the particles, and hence are strongly perturbed by the mechanical noise in the laboratory. The lower panels show the, near-zero, cross correlation functions between the eigenmodes.

the ring and periodic chain analyses give reasonable approximations to the real system and neither the finite particle size nor the geometric mapping of the ring onto the periodic chain lead to major deviations in the eigenmodes.

However, a more detailed examination of the eigenvalue spectrum, i.e., the damping rates of the eigenmodes, reveals some significant differences. Figure 4 shows the measured eigenvalues of the eigenmodes for the ring and a 1D periodic chain of eight particles. In both cases, to allow for slight measurement uncertainty in the magnification of the image, the precise geometry of the particles is scaled by a few percent to give best agreement between the predicted and observed highly damped modes. Many of these highly damped eigenmodes of the ring and periodic chain are similar or identical in form; not surprisingly, both analyses yield similar eigenvalues.

The largest discrepancies between the treatments occurs

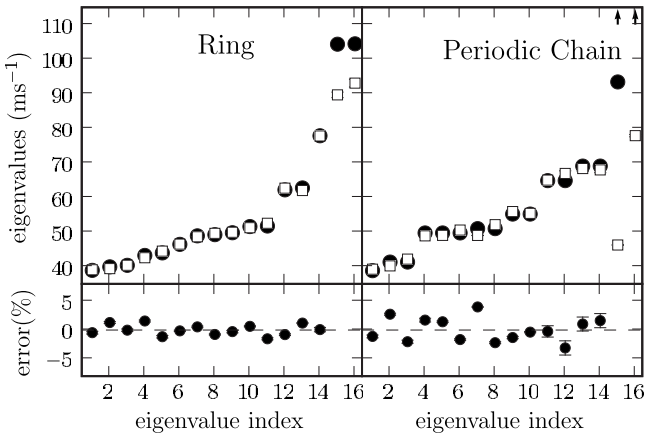

FIG. 4. Experimental (white squares) and predicted (black circles) decay rates for the eigenmodes of a ring and a 1D periodic chain of eight trapped particles subject to hydrodynamic coupling.

for eigenmodes 15 and 16 of the periodic chain whose corresponding eigenvalues, in the Oseen approximation, diverge as the logarithm of the chain length (strictly, for an infinite chain length these modes are undamped). Eigenmode 16, the common axial motion of the chain, maps onto azimuthal rotation, which is eigenmode 14 of the ring. Eigenmode 15, the common lateral motion of the chain, maps onto a radial stretch, which is eigenmode 6 of the ring. More generally we see that for the highly damped modes where hydrodynamic forces are dominated by nearest neighbor interactions, the agreement between analyses for the ring and the periodic chain is high. For the low damped modes in which neighboring particles move in similar directions, the forces between distance particles are more significant. In these cases coupling across the diameter of the ring perturbs the dynamics. The biggest discrepancy in the observations for the ring occurs for the common motion eigenmodes, which we suspect are perturbed by mechanical noise within the laboratory.

We have shown that a high-speed camera has sufficient measurement precision to accurately resolve the weak hydrodynamic coupling between an array of trapped particles. We have demonstrated the sensitivity of the technique by using it to analyze the eigenmodes of a trapped ring and consider how close an approximation these are to those of a periodic 1D chain. Though interparticle distances are only about three diameters, Oseen theory, applied to the ring, succesfully predicts the experimental eigenvalues to better than 2%. We find that the equivalence of ring and chain is superficially close but there are also differences. The most obvious difference arises for the modes with lowest damping, for which coupling between particles across the diameter of the ring becomes significant, increasing significantly the damping of these modes. Beyond applications in the study of hydrodynamic coupling, the high-precision, high-bandwidth multiparticle measurements made possible using these "smart cameras" opens the opportunity for multipoint photonic force microscopy [28].

[1] R. Larson, *The Structure and Rheology of Complex Fluids* (Oxford University Press, New York, 1999).

[2] A. Banchio, J. Gapinski, A. Patkowski, W. Häußler, A. Fluerasu, S. Sacanna, P. Holmqvist, G. Meier, M. Lettinga, and G. Nägele, Phys. Rev. Lett. **96**, 138303 (2006).

[3] A. Wille, F. Valmont, K. Zahm, and G. Maret, Europhys. Lett. **57**, 219 (2002).

[4] P. Keim, G. Maret, U. Herz, and H. H. von Grünberg, Phys. Rev. Lett. **92**, 215504 (2004).

[5] K. Zahn, A. Wille, G. Maret, S. Sengupta, and P. Nielaba, Phys. Rev. Lett. **90**, 155506 (2003).

[6] Q. Wei, C. Bechinger, and P. Leiderer, Science **287**, 625 (2000).

[7] B. Lin, B. Cui, J.-H. Lee, and J. Yu, Europhys. Lett. **57**, 724 (2002).

[8] C. Lutz, M. Kollmann, P. Leiderer, and C. Bechinger, J. Phys.: Condens. Matter **16**, S4075 (2004).

[9] G. Coupier, M. S. Jean, and C. Guthmann, Phys. Rev. E **73**, 031112 (2006).

[10] A. Ashkin, J. M. Dziedzic, J. E. Bjorkholm, and S. Chu, Opt. Lett. **11**, 288 (1986).

[11] J.-C. Meiners and S. R. Quake, Phys. Rev. Lett. **82**, 2211 (1999).

[12] E. R. Dufresne, T. M. Squires, M. P. Brenner, and D. G. Grier, Phys. Rev. Lett. **85**, 3317 (2000).

[13] F. Gittes and C. Schmidt, Opt. Lett. **23**, 7 (1998).

[14] C. D. Mellor, M. A. Sharp, C. D. Bain, and A. D. Ward, J. Appl. Phys. **97**, 103114 (2005).

[15] M. Polin, D. G. Grier, and S. R. Quake, Phys. Rev. Lett. **96**, 088101 (2006).

[16] W. H. Southwell, J. Opt. Soc. Am. **70**, 998 (1980).

[17] C. D. Saunter, G. D. Love, M. Johns, and J. Holmes, Proc. SPIE **6018**, 429 (2005).

[18] E. R. Dufresne and D. G. Grier, Rev. Sci. Instrum. **69**, 1974 (1998).

[19] J. Liesener, M. Reicherter, T. Haist, and H. J. Tiziani, Opt. Commun. **185**, 77 (2000).

[20] J. E. Curtis, B. A. Koss, and D. G. Grier, Opt. Commun. **207**, 169 (2002).

[21] G. Sinclair, P. Jordan, J. Courtial, M. Padgett, J. Cooper, and Z. J. Laczik, Opt. Express **12**, 5475 (2004).

[22] R. Di Leonardo, F. Ianni, and G. Ruocco, Opt. Express **15**, 1913 (2007).

[23] R. W. Gerchberg and W. O. Saxton, Optik (Jena) **35**, 237 (1972).

[24] B. C. Carter, G. T. Shubeita, and S. P. Gross, Phys. Biol. **2**, 60 (2005).

[25] S. Keen, J. Leach, G. Gibson, and M. J. Padgett, J. Opt. A, Pure Appl. Opt. **9**, S264 (2007).

[26] J. Brady and G. Bossis, Annu. Rev. Fluid Mech. **20**, 111 (1988).

[27] M. Doi and S. Edwards, *The Theory of Polymer Dynamics* (Oxford University Press, New York, 1986).

[28] A. Pralle, M. Prummer, E. L. Florin, E. H. K. Stelzer, and J. K. H. Hörber, Microsc. Res. Tech. **44**, 378 (1999).